

RESEARCH

Open Access



Human umbilical cord mesenchymal stem cells combined with pirfenidone upregulates the expression of RGS2 in the pulmonary fibrosis in mice

Xian Wu^{1,2,3}, Hao Gou⁴, Ou Zhou⁵, Huijun Qiu⁵, Hanmin Liu^{1,2,3}, Zhou Fu^{5,6,7*} and Lina Chen^{1,2,3*}

Abstract

Objective: The therapeutic effect of umbilical cord-derived mesenchymal stem cells (hUC-MSCs) in combination with pirfenidone (PFD) on pulmonary fibrosis in mice and its possible mechanism were investigated.

Methods: C57BL/6 mice were randomly divided into six groups: control group, model group, P₁₀ group, P₃₀ group, P₁₀₀ group, and P₃₀₀ group. Modeled by tracheal intubation with 3 mg/kg bleomycin drip, each dose of PFD was administered daily by gavage from day 7 onwards. The mice were observed continuously for 21 days and survival was recorded. Lung tissues were collected on day 21, and hematoxylin–eosin (HE) and Masson staining were performed to assess morphological changes and collagen deposition in the lungs. Collagen content was measured by the Sircol method, and fibrosis marker levels were detected by PCR and Western blot. Another batch of C57BL/6 mice was then randomly divided into five groups: hUC-MSC control group, model group, P₁₀₀ group, hUC-MSC treatment group, and hUC-MSCs + P₃₀ group. On day 7, 5 × 10⁵ hUC-MSCs were injected into the tail vein, the mice were administered PFD gavage daily from day 7 onwards, and their survival was recorded. Lung tissues were collected on day 21 to detect pathological changes, the collagen content, and the expression of regulator of G protein signaling 2 (RGS2). Pulmonary myofibroblasts (MFBs) were divided into an MFB group and an MFB + hUC-MSCs group; different doses of PFD were administered to each group, and the levels of RGS2, intracellular Ca²⁺, and fibrosis markers were recorded for each group.

Results: Compared with other PFD group doses, the P₁₀₀ group had significantly improved mouse survival and lung pathology and significantly reduced collagen and fibrosis marker levels ($p < 0.05$). The hUC-MSCs + P₃₀ group had significantly improved mouse survival and lung pathology, significantly reduced collagen content and fibrosis marker levels ($p < 0.05$), and the efficacy was better than that of the P₁₀₀ and hUC-MSCs groups ($p < 0.05$). RGS2 expression was significantly higher in the MSCs + P₃₀ group compared with the P₁₀₀ and hUC-MSCs groups ($p < 0.05$). PFD increased RGS2 expression in MFBs ($p < 0.05$) in a dose-dependent manner. Compared with PFD and hUC-MSCs treatment alone, combination of hUC-MSCs and PFD increased RGS2 protein levels, significantly decreased intracellular Ca²⁺ concentration, and significantly reduced fibrosis markers.

*Correspondence: fuzhoucqmu@126.com; chenln66@163.com

¹ Division of Pediatric Pulmonology and Immunology, West China Second University Hospital, Sichuan University, Chengdu 610041, Sichuan, China

⁶ Department of Respiratory Medicine, Children's Hospital of Chongqing Medical University, Chongqing 400015, China

Full list of author information is available at the end of the article



Conclusion: The findings suggest that hUC-MSCs combined with low-dose PFD have a therapeutic effect better than that of the two treatments used separately. Its effect on attenuating bleomycin-induced pulmonary fibrosis in mice is related to the increase of RGS2.

Background

Idiopathic pulmonary fibrosis (IPF), a diffuse inflammatory disease of the lower respiratory tract with unknown etiology, is a chronic interstitial lung disease characterized by progressive dyspnea and deterioration of lung function [1]. Its incidence increases every year; the median survival is only 2.5–3.5 years, and the prognosis is worse than that of many types of cancer [2, 3].

The 2015 edition of the clinical practice guidelines for the treatment of IPF states that the use of prednisone, azathioprine, N-acetylcysteine monotherapy, anticoagulants, platelet-derived growth factor receptor antagonists, endothelin receptor antagonists, and 5-phosphodiesterase inhibitors is strongly discouraged in patients with IPF, and that there are only four conditional recommended drugs, including pirfenidone (PFD), nintedanib, N-acetylcysteine combination therapy, and antacid therapy [1]. Although the emergence of PFD has benefited many IPF patients, in the 2015 edition of the clinical practice guidelines for the treatment of IPF, PFD was defined as a conditionally recommended drug due to its high effective dose, numerous adverse effects, and effectiveness only in mild-to-moderate IPF [1, 4, 5]. Therefore, the current monotherapy for PFD is not effective, so it is important to find an improved treatment.

Cell therapy based on stem cell technology has been a popular trend in recent years [6]. Human umbilical cord-derived mesenchymal stem cells (hUC-MSCs) are a type of adult stem cell with multi-directional differentiation potential derived from the mesoderm, and they are widely used because of the simplicity of their extraction, lack of ethical restrictions, strong immunomodulatory properties, and low immunogenicity [7, 8]. Clinical trials on hUC-MSCs for the treatment of various systemic diseases have been conducted worldwide, confirming the safety of hUC-MSCs in clinical applications [9–11]. Recent studies have shown that hUC-MSCs induce immune modulation and inflammation control through paracrine secretion of multiple factors and microvesicles, which can reduce profibrotic factors and collagen deposition, producing therapeutic effects in animal models of bleomycin-induced early pulmonary fibrosis [12, 13]; however, hUC-MSCs offer limited therapeutic effects in the late stage of pulmonary fibrosis [14].

RGS2 is a suppressor of G protein-coupled proteins that has received increasing attention in fibrotic diseases

[15–17]. Recent studies have found that RGS2 expression is significantly downregulated in animal models of renal fibrosis and cardiac hypertrophy, suggesting that RGS2 plays an important role in regulating the pathogenesis of fibrosis [18, 19]. Enhanced RGS2 expression protects against pulmonary fibrosis in mice, while knockdown of RGS2 promotes fibrosis in mice, which demonstrates that endogenous RGS2 has an antifibrotic function and that RGS2 is the basis of the antifibrotic effect of PFD [20]. However, the biological function of RGS2 in bleomycin-induced pulmonary fibrosis in mice and its mechanism of action are rarely reported in the literature.

In this study, we established a mouse model of pulmonary fibrosis using bleomycin to investigate the effects of hUC-MSCs combined with low-dose PFD by observing the survival rate and lung pathological changes and by detecting the expression level of pulmonary fibrosis markers in the mice. PFD and hUC-MSCs were combined to act on myofibroblasts (MFBs) to observe the effect of their combination on the expression of RGS2, which has antifibrotic effects, to preliminarily explore the possible mechanism of the combined treatment and provide a theoretical basis for the treatment of IPF with hUC-MSCs combined with PFD.

Methods

Animal grouping and treatment

SPF-grade 7-week-old C57BL/6 male rats were purchased from the Animal Experiment Center of Chongqing Medical University and housed in an SPF-grade breeding room at 22–26 °C, 55–60% humidity, and 12 h/day light rotation; modeling was started after 1 week of adaptation.

We divided 60 C57BL/6 rats into 6 groups using the random number method: control group (N), bleomycin model group (B), P₁₀ group (10 mg/kg PFD, P₁₀), P₃₀ group (30 mg/kg PFD, P₃₀), P₁₀₀ group (100 mg/kg PFD, P₁₀₀), and P₃₀₀ group (300 mg/kg PFD, P₃₀₀). The pulmonary fibrosis model was established by dripping bleomycin 3 mg/kg into the lungs of mice at an equal rate through tracheal intubation, and the control group was administered an equal amount of saline at an equal rate. After successful modeling, each PFD dose group was administered 10 mg/kg, 30 mg/kg, 100 mg/kg, or 300 mg/kg PFD (Adamas Reagents, China) suspension by gavage from day 7 after modeling, and the control group

was administered an equal volume of saline once per day until day 21 after modeling.

Another batch of 60 C57BL/6 mice was divided into 6 groups using the random number method: control group (N), hUC-MSCs control group (N + M), bleomycin model group (B), hUC-MSCs treatment group (B + M), P₁₀₀ group (100 mg/kg PFD, P₁₀₀), and hUC-MSCs + P₃₀ group (hUC-MSCs + 30 mg/kg PFD, B + M + P₃₀). Modeling was performed by tracheal intubation with 3 mg/kg bleomycin drip, and on day 7 after modeling, hUC-MSCs control and hUC-MSCs treatment groups were injected with $5 \times 10^5/200 \mu\text{L}$ P₄ generation hUC-MSCs via the tail vein of mice, and the non-MSC group was injected with an equal amount of saline. Starting from day 7 after modeling, the P₁₀₀ group and the hUC-MSCs + P₃₀ group (B + M + P₃₀) were administered 100 mg/kg and 30 mg/kg PFD suspension by gavage, respectively, and the control group was administered an equal volume of saline once daily until day 21 after modeling. The survival of the mice was recorded, and lung tissues were collected on day 21. The mice survival curves, analysis of lung histopathology, determination of lungs collagen content, detection of mRNA, markers of lung fibrosis, and detection of RGS2 expression will be described briefly.

Survival curves

The survival of each group of mice was observed and recorded, and survival curves were plotted using GraphPad Prism 5.0.

Lung histological analysis

Paraformaldehyde-fixed mouse lung sections were analyzed with hematoxylin–eosin (HE) or Masson's trichrome staining (Leagene Biotechnology, China) to assess fibrotic changes in the lungs. Three anterior, middle, and posterior sections of each lung specimen of mice were harvested for HE and Masson staining, and five high-magnification views of each section were then selected for observation and scored separately using the modified Ashcroft method (scale range 0 to 8) [21]. The histopathological score of pulmonary fibrosis for each mouse was expressed as the mean score of the sections.

Determination of intrapulmonary collagen content

We took 80 mg of lung tissue from the right lung according to the Sircol method (Biocolor, UK) for measuring soluble collagen. A standard curve was produced using collagen standards, and the collagen concentration was calculated from the standard curve. Soluble collagen content was calculated according to the following formula: soluble collagen content = calculated collagen concentration \times total volume of hydrolysate (1 mL)/80 mg \times total wet weight of right lung tissue \times 1000 (μg).

Fluorescence quantitative PCR

Total RNA was extracted from each group of lung tissues using the TRIZOL method, and the RNA was reverse-transcribed into cDNA using a reverse transcription kit (Takara, Japan). The primers, including β -actin, type I collagen $\alpha 1$ (Col1a1), type I collagen $\alpha 2$ (Col1a2), α -smooth muscle actin (α -SMA), RGS2, calcium adhesion protein E (E-cad), and fibronectin (FN) were synthesized by Chengdu Kengke Zixi Biotechnology Co. Ltd. The cDNA was used for fluorescence quantitative PCR, and the expression of Col1a1, Col1a2 and α -SMA, RGS2, E-cad, and FN was detected using the β -actin gene as the internal reference gene level. The genes, mRNA, and protein are referred to using official gene symbols, as provided by the National Center for Biotechnology Information (NCBI; <https://www.ncbi.nlm.nih.gov>).

Western blot

Protein was extracted from lung tissue using RIPA lysis buffer (Beyotime Biotechnology, China). Samples were electrophoresed and subjected to Western blot analysis using a primary antibody against RGS2 (Santa Cruz Biotechnology, RGS2 BC-43, sc-100761) and β -actin. Anti-mouse secondary antibodies (ZSGB Biotechnology, China) were used to capture images with chemiluminescence and fluorescence systems (Syngene U.S.).

Acquisition and identification of hUC-MSCs

P₂ generation hUC-MSCs were obtained from Chongqing Stem Cell Therapy Engineering Technology Research Center. The hUC-MSCs were cultured and identified according to the methods reported in the literature [22, 23]. The hUC-MSCs were grown to P₄ generation; cell suspensions were collected after trypsin digestion, centrifuged, and resuspended with PBS and counted to a final cell concentration of $2.5 \times 10^6/\text{mL}$ then placed on ice for use.

Acquisition, grouping and treatment of myofibroblasts

P₄ generation NIH3T3 and HLF-9 were spread in six-well plates (Corning, USA) at 1×10^6 in a humidified incubator at 37 °C with 5% CO₂. When the cell fusion reached approximately 80%, they were replaced with fresh DMEM (Gibco, USA) medium containing 1% FBS (Gibco, USA), treated with 4 ng/ml transforming growth factor- $\beta 1$ (TGF- $\beta 1$, Peprotech USA), and cultured for 24 h (i.e., MFBs of both cell lines). Different concentrations of PFD were added to the MFBs: 0, 2, 4, 6, 8, and 10 mM. The cells in each group were collected after 2 h of incubation, and RGS2 mRNA expression was detected by RT-PCR to determine the effective increase in concentration of RGS2 mRNA caused by PFD. The effective concentration of PFD was added to the MFBs separately, the

cells in each group were collected separately after 24 h of culture, and the mRNA expression of fibrosis markers was detected by RT-PCR.

The cells were divided into three groups according to different culture methods: NIH3T3 group (N+T) or HLF-9 group (H+T), hUC-MSCs group (M+T), and NIH3T3+hUC-MSCs group (N+T+M) or HLF-9+hUC-MSCs group (H+T+M). NIH3T3 or HLF-9 were cultured in the lower chamber of one well of the six-well co-culture plate alone (N or H). The P₄ generation hUC-MSCs were cultured in the upper chamber of the other well of the six-well co-culture plate (M+T). MFBs were cultured in the lower chamber of the six-well co-culture plate, and P₄ generation hUC-MSCs were cultured in the upper chamber of the six-well co-culture plate (N+T+M or H+T+M). All cells were cultured using DMEM/F12 (Gibco, USA) containing 5% FBS. When the cell fusion of each group reached approximately 80%, the effective concentration of PFD or equal amount of PBS buffer was added, each group of cells was collected after 24 h of culture, and the mRNA expression of RGS2 and fibrosis markers was detected by RT-PCR.

The hUC-MSCs were divided into three groups: hUC-MSCs group (M), hUC-MSCs+TGF-β1 group (M+T), and hUC-MSCs+TGF-β1+PFD group (M+T+P). The hUC-MSCs were cultured using DMEM/F12 containing 5% FBS, and when the fusion of cells in each group reached approximately 80%, they were replaced with fresh DMEM containing 1% DMEM medium with FBS, treated with 4 ng/ml TGF-β1, and cultured for 24 h. Cells in the M+T group were collected and detected by RT-PCR for E-cad, FN, and α-SMA mRNA expression. In the M+T+P group, PFD or an equal amount of PBS buffer was added after 24 h of TGF-β1 treatment, and the cells were collected after 24 h of culture and detected by RT-PCR for E-cad, FN, and α-SMA mRNA expression.

Measurement of intracellular Ca²⁺

HLF-9 and NIH3T3 seeded into 6-well plates at 1×10^4 cells/well and treated with or without PFD and hUC-MSCs were removed from the incubator. Culture solution was removed, the cells were rinsed 3 times with HEPES and 5 mM Fluo-3/AM (Beyotime Biotechnology, China) according to kit instructions was added. Next, HLF-9 and NIH3T3 were incubated at 37 °C for 40 min, followed by 3 washes with HEPES to discard the remaining extracellular probe and HEPES culture medium was used to cover all cells in the troughs. Laser scanning confocal microscopy (LSCM) was performed to observe the fluorescence intensity (FI) of the cells, using an excitation wavelength of 488 nm and emission wavelength of 530 nm.

RNA interference

We used interfering RNA (siRNA) to examine the functional consequences of downregulation of endogenous RGS2. The siRNA for RGS2 was previously generated with AAGGAAAATATACACCGACTT as target sequence for the RNA interference experiments [24]. Confusing siRNA sequences derived from the designed siRNA sequences were used as negative controls. The siRNA sequence was synthesised by Shanghai Tuo Ran Biological Technology Co., Ltd. NIH3T3 was inoculated in 6-well plates one day before transfection, and complete medium (DMEM/F12 with 10% FBS) was added to each well. Before transfection, siRNA and lipfectmaineTM2000(lip2000, Invitrogen, USA) were diluted separately with serum-free medium Opti-MEM[®] I (Gibco, USA) and then gently mixed and incubated for 20 min at room temperature. The siRNA-lip2000 mixture was added to NIH3T3 in 6-well plates and incubated under normal conditions (37 °C and 5% CO₂) for 6 h. The medium containing siRNA-lip2000 mixture in the wells was removed and replaced with complete medium to continue incubation under normal conditions. One group of cells was used to detect cell activity, and the other group was cultured for 48 h. Cells were collected first for counting and then protein extraction, and the expression level of RGS2 within siRNAs and controls were used to detect by Western blot and QT-PCR.

Statistical analysis

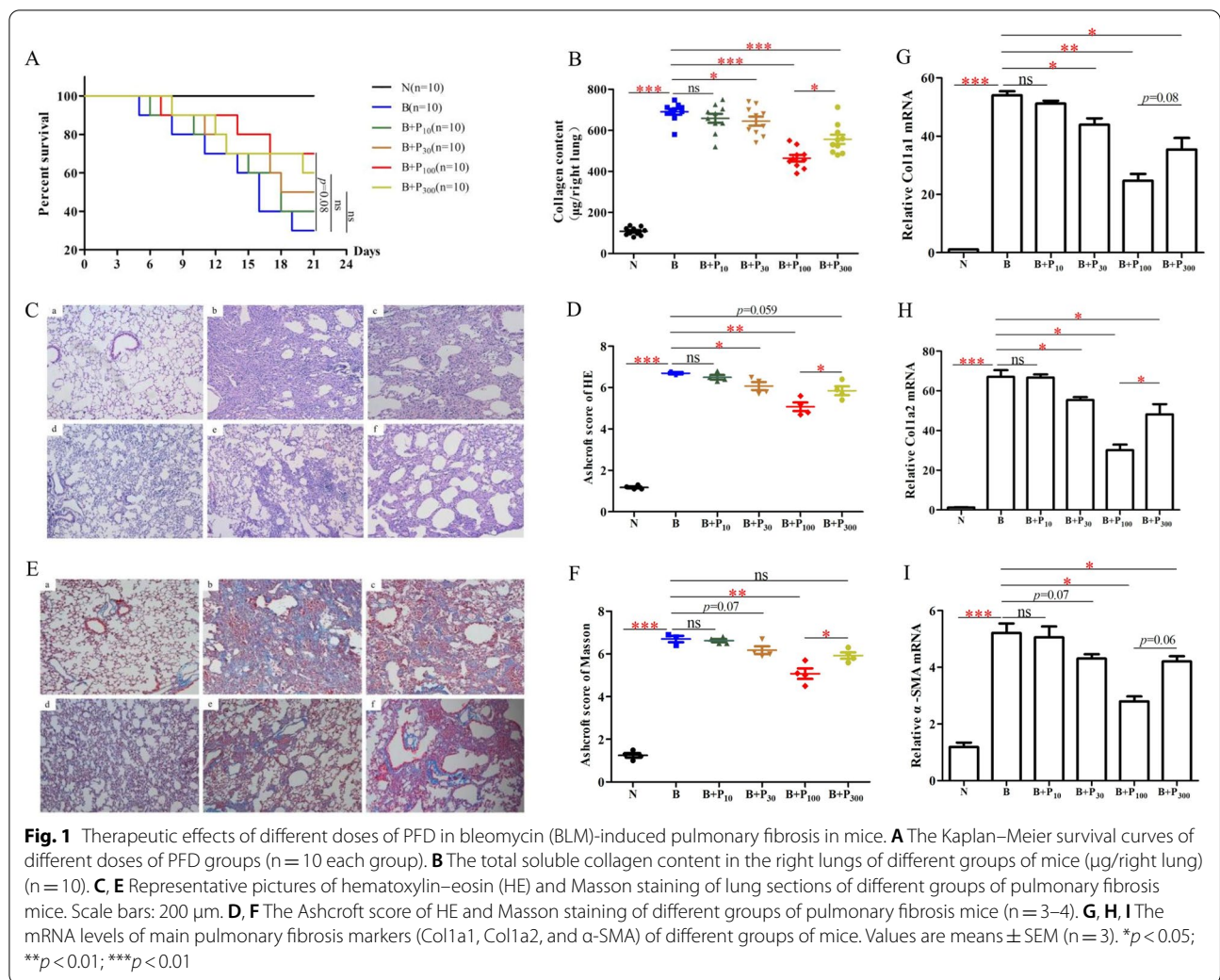
Data are expressed as means ± SEM. Comparisons between groups were made using Student's t test for unpaired observations or two-factor ANOVA and Bonferroni correction for multiple comparisons. $p < 0.05$ was considered statistically significant.

Results

Therapeutic effects of different doses of PFD in BLM induced pulmonary fibrosis mice

Compared with the survival time in the model group (B), the low dose of PFD (10 mg/kg, P₁₀) alone could not prolong the survival time of mice with pulmonary fibrosis, and there was a trend to prolong the survival time in the low-dose group (30 mg/kg, P₃₀), the medium-dose group (100 mg/kg, P₁₀₀), and the high-dose PFD (300 mg/kg, P₃₀₀) alone; however, the differences were not significant ($p = 0.38$, $p = 0.08$, $p = 0.19$, respectively, $n = 10$ each group) (Fig. 1A). Detailed survival of mice is shown in Additional file 1: Table S1.

Using the Sircol method, we detected the soluble collagen content in the lungs of mice ($n = 10$), and the collagen content of the right lungs of mice in the model



group was significantly higher than in the control group ($p < 0.001$). Compared with the model group, the right lung collagen content of the P₁₀ group did not significantly change, the collagen content of the P₃₀ group was significantly reduced ($p < 0.05$), the collagen content of the P₁₀₀ group was significantly reduced ($p < 0.001$), and the collagen content of the P₃₀₀ group was significantly reduced ($p < 0.001$); however, the reduction was not as great as that of the P₁₀₀ group ($p < 0.05$) (Fig. 1B).

The pathological changes in the mice of the model group on day 21 of modeling were (n = 3–4): inflammatory cell exudation, widening of alveolar septa, formation of a ground glass-like, strip-like, grid-like structure at the base of both lungs, and cystic changes of varying sizes in some areas (i.e., honeycomb lung). Compared with the lung pathology of the model group, there was no significant improvement in the P₁₀ group, a trend of improvement in the P₃₀ group ($p = 0.055$), a decrease in the areas of lattice-like and honeycomb shape in the lungs of the

P₁₀₀ group, and a significant improvement of the Ashcroft score ($p < 0.001$). There was some improvement in the lung pathology of the P₃₀₀ group ($p = 0.059$), but less than that of the P₁₀₀ group ($p < 0.05$) (Fig. 1C, D). Masson staining colored the collagen in the lungs blue, which reflected the severity of fibrosis in the lungs. A large amount of collagen deposition in the lung was visualized microscopically in the model group. Compared with the model group, there was no significant change in intrapulmonary collagen deposition in the P₁₀ group; collagen deposition was significantly reduced in the P₃₀, P₁₀₀, and P₃₀₀ groups, but the collagen reduction in the P₃₀ and P₃₀₀ groups was not as great as that in the P₁₀₀ group ($p < 0.05$) (Fig. 1E, F).

Col1a1, Col1a2, and α-SMA are considered the main pulmonary fibrosis markers, and their levels reflect the degree of pulmonary fibrosis [25]. Col1a1 and Col1a2 mRNA levels were significantly higher in the model group than in the control group. Compared with the

model group, there was no significant change in Col1a1 mRNA in the P₁₀ group, and the expression of Col1a1 mRNA was significantly reduced in the P₃₀, P₁₀₀, and P₃₀₀ groups (Fig. 1G). Col1a2 mRNA levels were reduced in all treatment groups except for the low-dose PFD P₁₀ group ($p < 0.05$, $n = 3$), and the most significant reduction in Col1a2 mRNA expression was observed in the P₁₀₀ group ($p < 0.05$, $n = 3$). Compared with the α -SMA mRNA level in the model group, there was no significant change in the levels in the P₁₀ group, a decreasing trend was observed in the P₃₀ and P₃₀₀ groups ($p = 0.07$ and $p = 0.06$, respectively, $n = 3$), and a significant decrease was observed in the P₁₀₀ group ($p < 0.05$, $n = 3$) (Fig. 1I). Low-dose PFD (30 mg/kg) was the lowest effective dose for anti-fibrosis, medium-dose PFD (100 mg/kg) had the best efficacy among the groups with PFD alone, and high-dose PFD (300 mg/kg) was not as effective as medium-dose PFD for anti-fibrosis.

Culture and characterization of hUC-MSCs

hUC-MSCs cultured in DMEM/F12 medium at 37 °C in a 5% CO₂ incubator were assayed for surface-specific antigens of P₄ generation hUC-MSCs using flow cytometry. The results showed that the surface molecules CD34, CD45, and the HLA-DR positivity of hUC-MSCs were less than 2%, and CD73, CD90, and CD105 positivity were higher than 95% (Fig. 2A, Additional file 1: Fig. S1). This observation is in accordance with the standards published by the International Stem Cell Therapy Association in 2006. In addition, we examined the multidirectional differentiation potential of hUC-MSCs; our results showed that hUC-MSCs differentiated into chondrogenic (Fig. 2B, Additional file 1: Fig. S2A), osteogenic (Fig. 2C, Additional file 1: Fig. S2B), and adipogenic cells (Fig. 2D, Additional file 1: Fig. S2C).

Therapeutic effects of hUC-MSCs combined with P₃₀ in BLM induced pulmonary fibrosis mice

Studies have shown that hUC-MSCs can attenuate acute lung injury and early pulmonary fibrosis; however, their therapeutic effect on established pulmonary fibrosis is unclear [13–15]. Preliminary experimental data from our group showed that hUC-MSCs administered alone by transcatheter tail vein injection were less effective in treating a mouse model of pulmonary fibrosis [19, 20]; therefore, the therapeutic effect of hUC-MSCs in combination with PFD on middle- and late-stage pulmonary fibrosis is unclear. In contrast, the efficacy of high doses of PFD was also not satisfactory and was associated with significant adverse effects. Therefore, we explored the therapeutic effect of hUC-MSCs combined with the lowest effective dose of PFD (30 mg/kg, P₃₀) on pulmonary fibrosis in mice. The results showed that hUC-MSCs

combined with P₃₀ significantly prolonged the survival time of the mice (Fig. 3A, $p < 0.05$, $n = 10$), and the survival time of the hUC-MSCs combined with P₃₀ group was longer than that of the P₁₀₀ group ($p = 0.07$). Detailed survival of mice is shown in Table. S2. The combination group had significantly reduced collagen content in the lungs ($p < 0.001$, $n = 10$), and the collagen content was significantly lower than that in the P₁₀₀ group (Fig. 3B, $p < 0.001$). Moreover, the combination group significantly improved bleomycin-induced pulmonary lesions, with significantly better Ashcroft scores ($p < 0.001$) and significantly reduced intrapulmonary collagen deposition, all with better improvement than P₁₀₀ (Fig. 3C–F, $p < 0.01$, $n = 4$). Regarding the expression of pulmonary fibrosis markers, Col1a1, Col1a2, and α -SMA mRNA levels were significantly decreased in the hUC-MSCs combined with the P₃₀ group compared with the model group (Fig. 3G–I, $p < 0.01$, $n = 3$), where the reduced levels of Col1a1 and Col1a2 were significantly different compared to the P₁₀₀ group alone, while the levels of α -SMA compared to the P₁₀₀ group tended to be lower ($p = 0.09$).

hUC-MSCs combined with low-dose P₃₀ elevated RGS2 mRNA and protein expression levels in mouse lung tissue

Studies have suggested that RGS2 is a novel mechanism explaining the antifibrotic effect of PFD [4]. Quantitative RT-PCR analysis in our study confirmed that, as expected, treatment of pulmonary fibrosis in mice with the optimal effective dose of PFD (100 mg/kg) increased RGS2 mRNA levels in mouse lung tissues (Fig. 4A, $p < 0.05$, $n = 3$), and RGS2 mRNA levels in the hUC-MSCs combined with P₃₀ group were more elevated than those in the P₁₀₀ group ($p < 0.05$, $n = 3$). Furthermore, Western blot analysis confirmed that RGS2 protein levels in lung tissue were significantly increased after PFD treatment in mice (Fig. 4B, C, $n = 3$), and RGS2 protein levels in the hUC-MSCs combined with P₃₀ group were higher than in the P₁₀₀ group.

RGS2 mRNA and protein expression levels in myofibroblasts

Studies have shown that MFBs are the main cells of tissues after fibrosis [26] and that TGF- β 1 induces the conversion of fibroblasts to MFBs [27]. In this experiment, two fibroblast model cells, MFBs, were obtained after stimulation of two fibroblast lines, NIH3T3 and HLF-9, for 24 h using 4 ng/mL TGF- β 1. hUC-MSCs and PFD in subsequent experiments were added to fibroblasts after TGF- β 1 stimulation.

Quantitative RT-PCR analysis confirmed that RGS2 mRNA was elevated in a concentration-dependent manner after PFD treatment of both MFBs (Fig. 4D, E), and

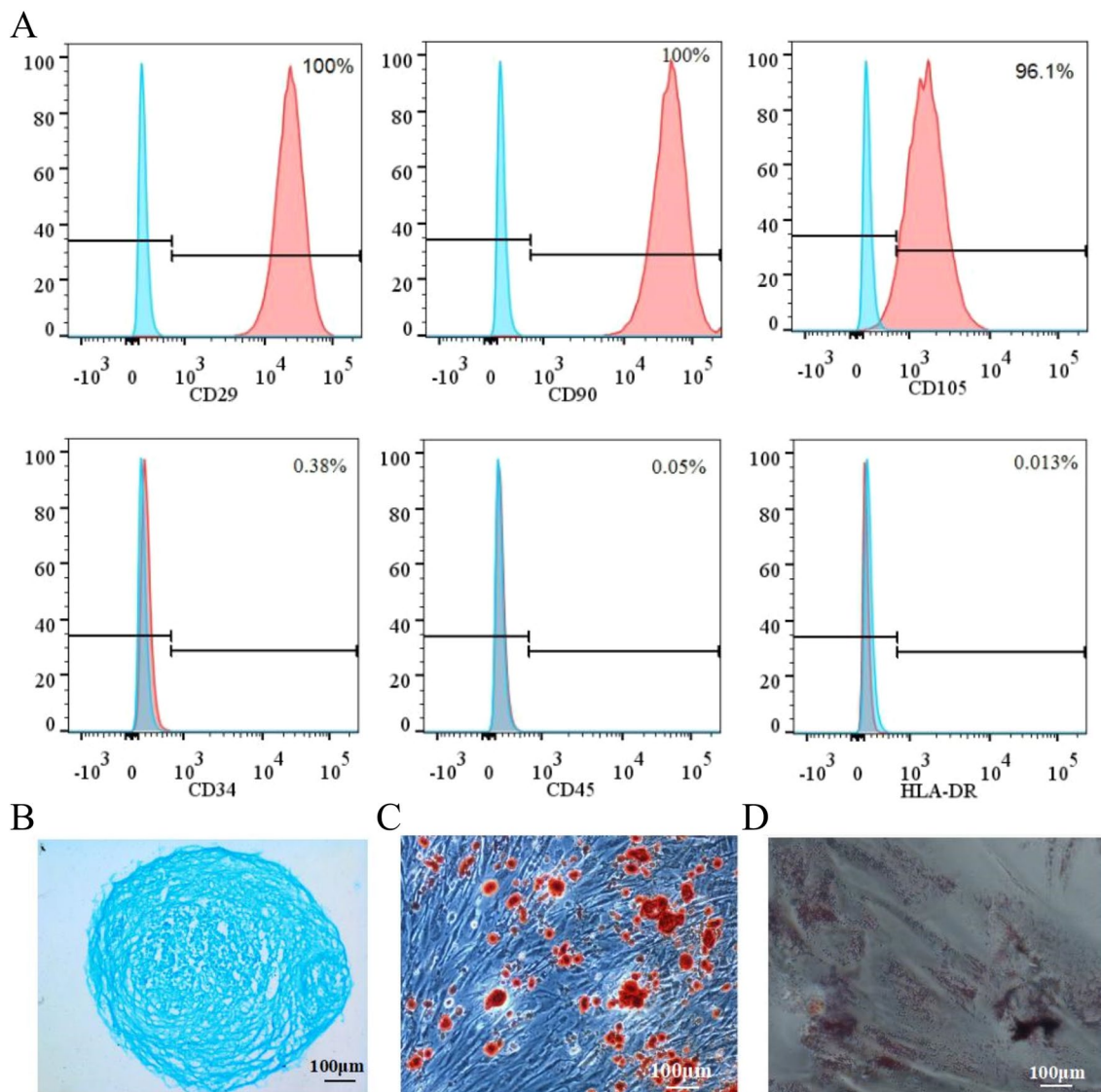


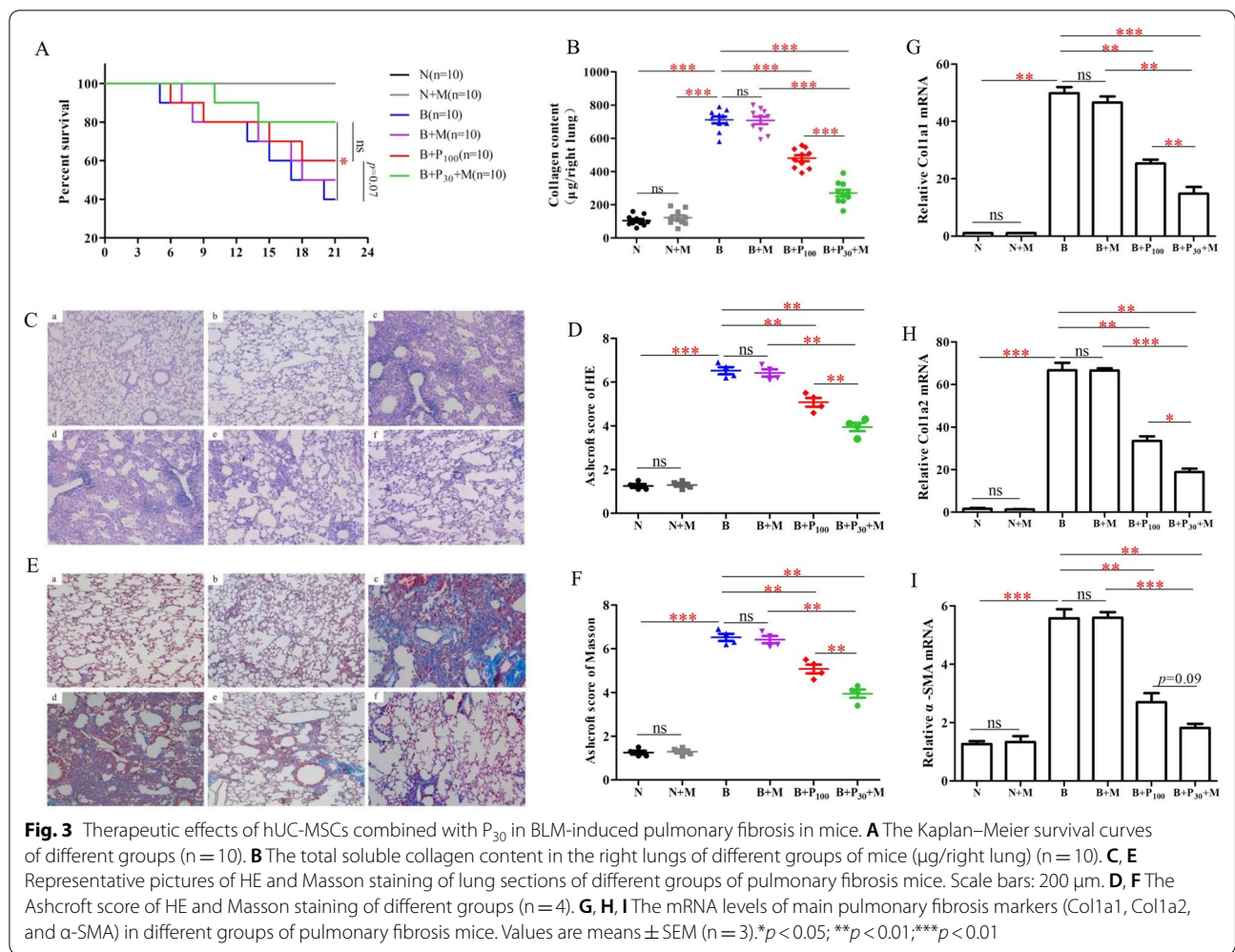
Fig. 2 The pluripotency of hUC-MSCs. **A** The expression of the surface markers CD34, CD45, HLA-DR, CD73, CD90, and CD105 in hUC-MSCs detected by flow cytometry. **B, C, D** The results of hUC-MSC differentiation into chondrocytes, osteocytes, and adipocytes. **B** Alcian blue staining of hUC-MSCs after 24-day culture. **C** Alizarin red staining of hUC-MSCs after 20-day culture. **D** Oil Red O staining of hUC-MSCs after 15-day culture

the elevation of RGS2 mRNA in both MFBs treated with ≥ 6 mM PFD was significant ($p < 0.05$). As shown in Fig. 4F and G, the mRNA of fibrosis markers in both MFBs decreased significantly after 24 h of PFD treatment ($n = 3$).

hUC-MSCs can affect the expression of RGS2 and the markers of pulmonary fibrosis of myofibroblasts by PFD treatment

The effect of PFD (8 mM) on the expression of RGS2 and lung fibrosis markers in MFBs was explored after co-culture of hUC-MSCs with MFBs. The results showed that the differences in RGS2 mRNA levels were significant in

the H + T + M + P group compared with the H + P group (Fig. 5A, $p < 0.01$, $n = 3$), as well as in the N + T + M + P group compared with the N + T + P group (Fig. 5E, $p < 0.05$, $n = 3$), indicating that hUC-MSCs further elevated RGS2 mRNA after co-action of MFB with PFD. Representative Western blot analysis of RGS2 protein expression was performed in HLF-9 (Fig. 5B) and NIH3T3 (Fig. 5F) without or with hUC-MSCs and/or PFD treatment. As shown in Fig. 5C and G, quantification of RGS2 expression is presented as means \pm SEM. The results demonstrated that RGS2 protein levels were statistically significant in the H + T + M + P group compared with



the H + T + P group and H + T + M group (Fig. 5C, p < 0.001), as well as in the N + T + M + P group compared with the N + T + P group and N + T + M group (Fig. 5G, p < 0.05). PFD can attenuate thrombin-induced increases in intracellular Ca²⁺ by upregulating RGS2 [4]. The intracellular Ca²⁺ increased induced by TGF-β1 [28]. In our study, intracellular Ca²⁺ levels in each group were measured, and we found that intracellular Ca²⁺ concentrations were reduced in the hUC-MSCs combined with PFD group (Fig. 5D, H). The Fluo-3 fluorescence intensity of intracellular Ca²⁺ in HLF-9 and NIH3T3 are shown in Additional file 1: Figs. S3 and S4 (n = 3). Co-treatment of MFBs with PFD and hUC-MSCs resulted in a significant decrease in fibrosis marker mRNA in both MFBs (Fig. 5I, J, n = 3).

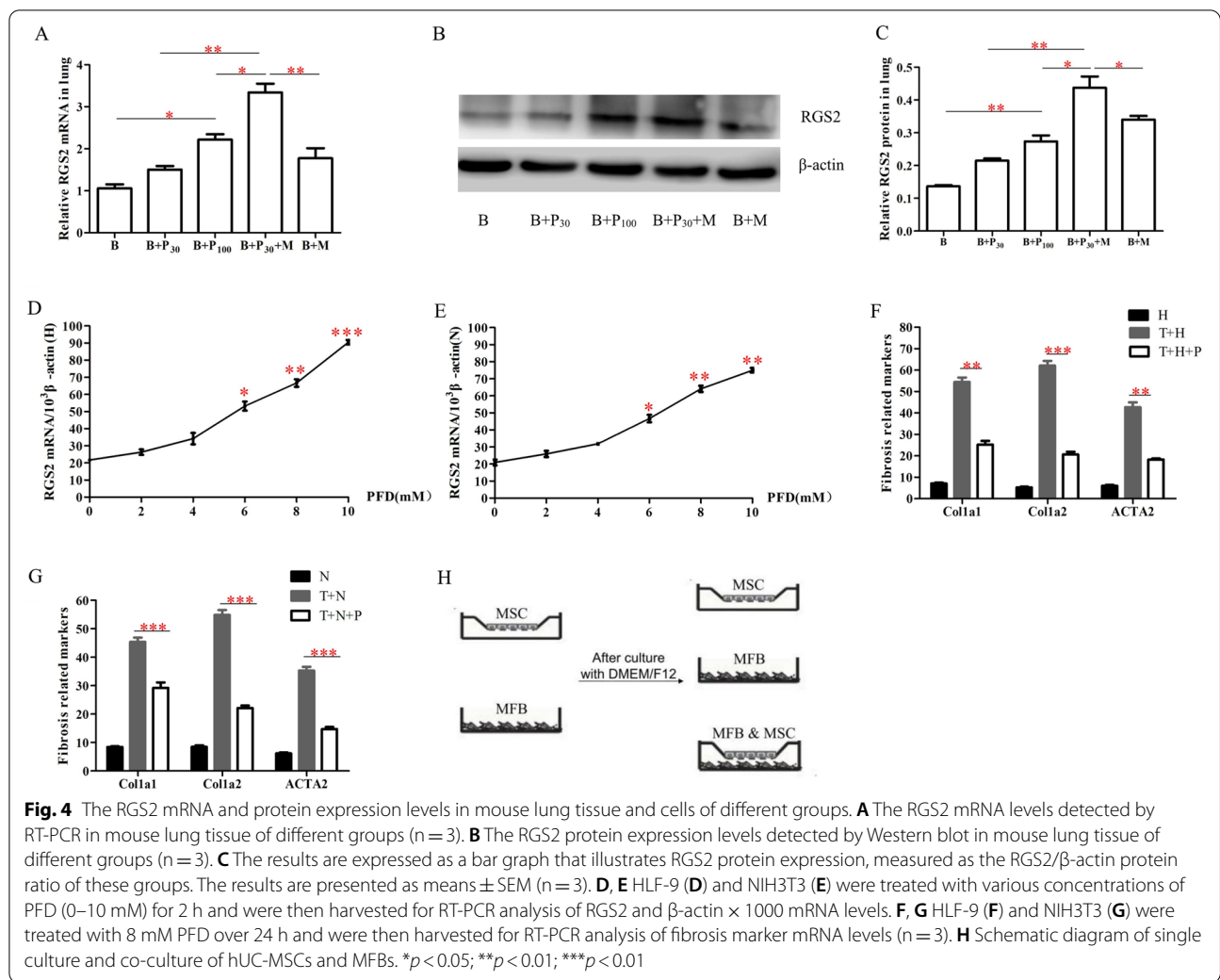
Furthermore, we examined the changes in mRNA levels of endothelial–mesenchymal transition (EMT) markers in hUC-MSCs. The results showed that E-cad mRNA was significantly increased, and both FN and α-SMA mRNA

expression were significantly decreased after treatment of hUC-MSCs with 8 mM PFD (Fig. 5k, p < 0.05, n = 3).

RGS2 knockdown enhances TGF-β1-induced pro-fibrotic effects in fibroblasts.

To investigate the effect of RGS2 downregulation on pulmonary fibrosis, NIH3T3 cells treated with TGF-β1 were transfected with RGS2-targeting siRNA and then cultured in vitro. Representative images of NIH3T3 transfected with or without siRNA show there are no apparent changes in cell viability (Fig. 6A). The number of NIH3T3 was almost equal between RGS2-siRNA-transfected and control groups (Fig. 6B, p > 0.05). Compared with cells transfected with control group, the RGS2 protein expression significantly decreased after transfection with RGS2-siRNA (Fig. 6C). In addition, we were able to achieve up to about 62% reduction in RGS2 mRNA (Fig. 6D).

Consistent with previous data, PFD alone treatment and hUC-MSCs in combination with PFD both



reduced the increase in TGF- β 1-induced fibrosis markers (Coll1a1, Coll1a2, and α -SMA). Importantly, reduction in RGS2 expression markedly enhanced TGF- β 1-induced pro-fibrotic effects in NIH3T3 (Fig. 6E–G). In marked contrast, PFD treatment had no effect in RGS2-siRNA-NIH3T3, indicating that upregulated RGS2 is a important mediator of the anti-fibrotic effects associated with PFD treatment (Fig. 6E–G). hUC-MSCs combined with PFD.

could reduce the expression of fibrosis markers to some extent, especially Coll1a2, but there was no statistical difference ($p > 0.05$).

Discussion

Although PFD has been approved by the Food and Drug Administration (FDA) for the treatment of IPF, its therapeutic effects are limited, and its adverse effects are large. In the present study, we used hUC-MSCs combined with

low-dose PFD for the treatment of pulmonary fibrosis in mice. We found that, combined with hUC-MSCs, low-dose PFD could exert antifibrotic effects superior to its threefold or even tenfold dose alone. Therefore, the findings suggest that the combination of hUC-MSCs and PFD can enhance the antifibrotic efficacy of PFD, reduce the required dosage of PFD, and decrease the incidence of adverse effects to enhance the tolerability and compliance of IPF patients.

Hisashi O et al. used concentrations of 10, 30, and 100 mg/kg PFD to treat a mouse model of bleomycin-induced pulmonary fibrosis, and the results of the study showed that the antifibrotic effect of PFD was positively correlated with the dose [29]. However, the efficacy of PFD containing higher dose gradients on pulmonary fibrosis in mice was not reported in this literature. In our present study, four dose gradients of 10, 30, 100, and 300 mg/kg PFD were applied to explore the therapeutic

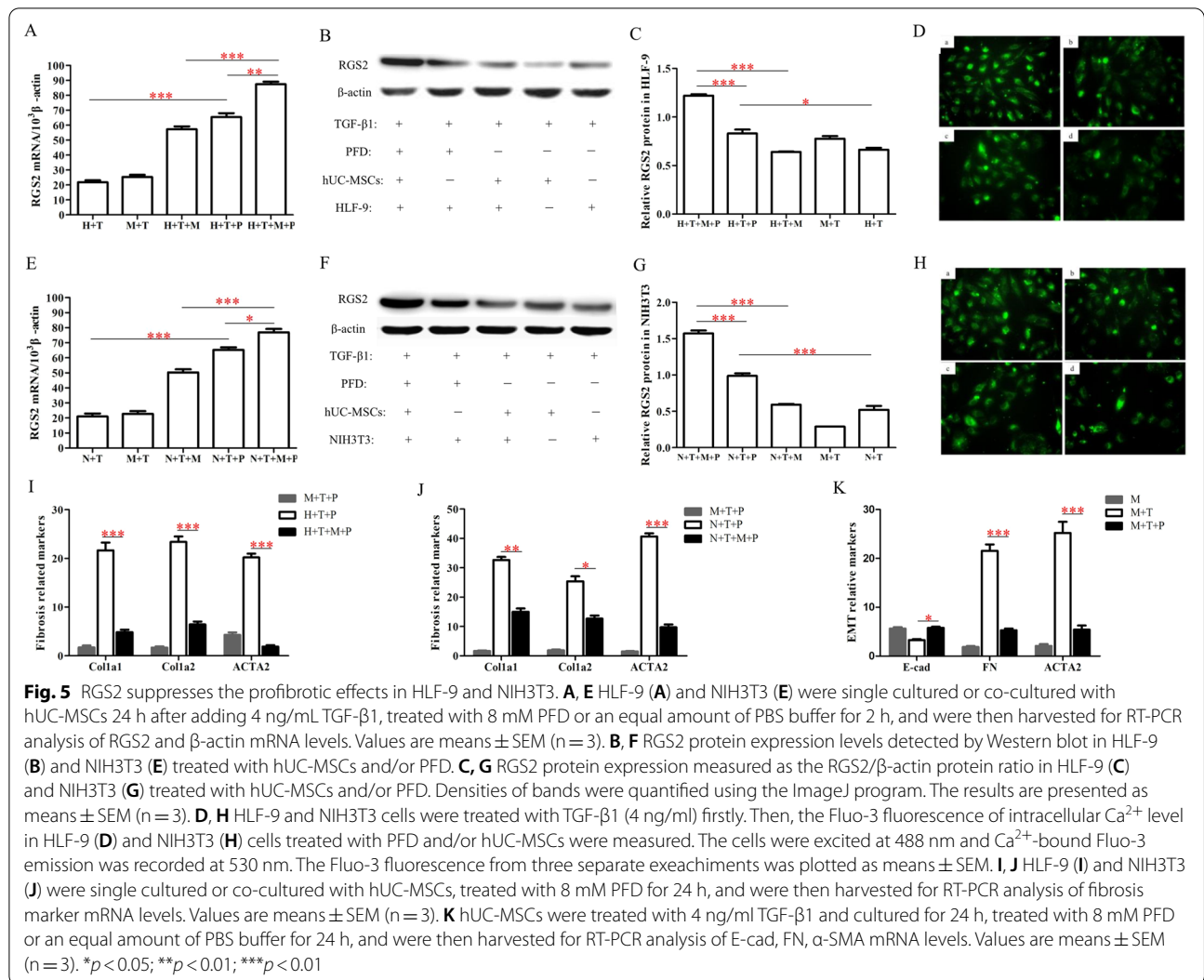
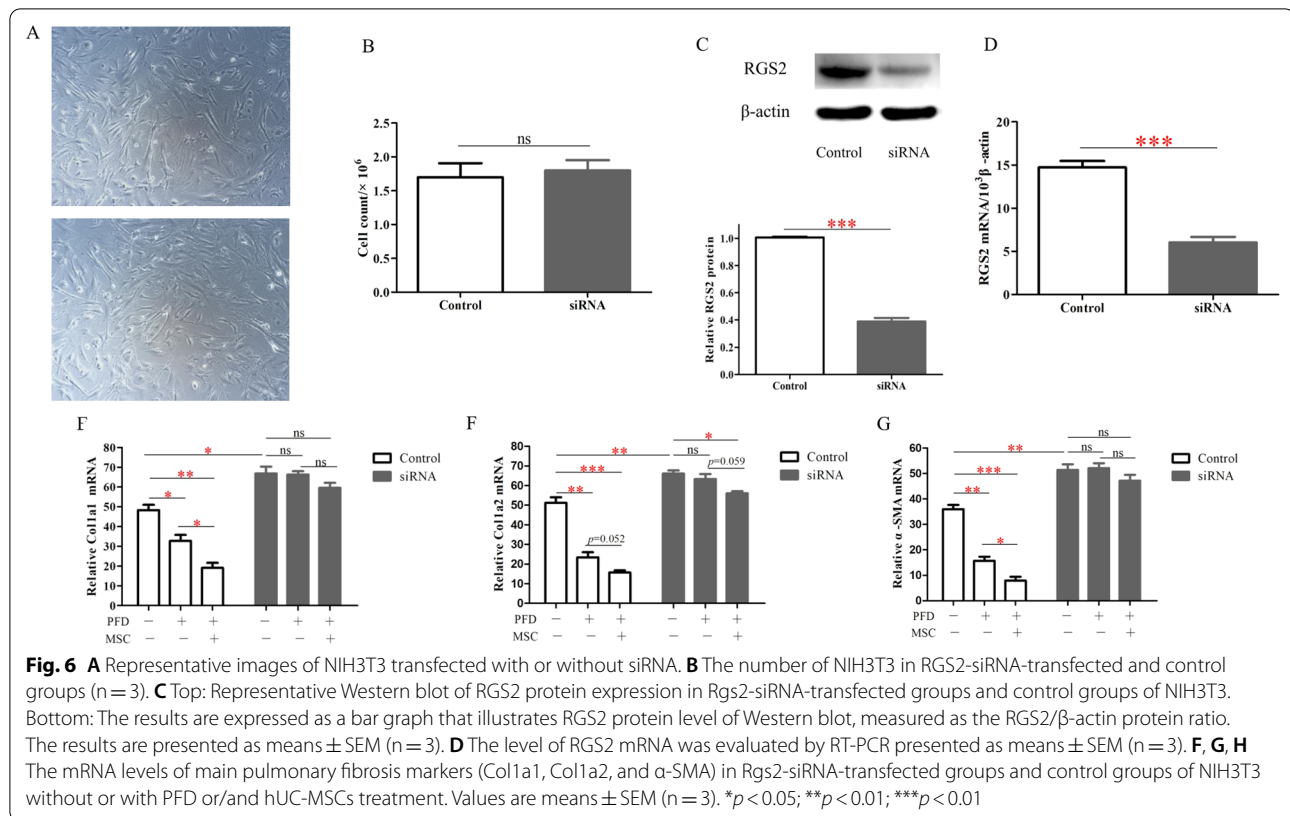


Fig. 5 RGS2 suppresses the profibrotic effects in HLF-9 and NIH3T3. **A, E** HLF-9 (**A**) and NIH3T3 (**E**) were single cultured or co-cultured with hUC-MSCs 24 h after adding 4 ng/mL TGF-β1, treated with 8 mM PFD or an equal amount of PBS buffer for 2 h, and were then harvested for RT-PCR analysis of RGS2 and β-actin mRNA levels. Values are means ± SEM (n = 3). **B, F** RGS2 protein expression levels detected by Western blot in HLF-9 (**B**) and NIH3T3 (**F**) treated with hUC-MSCs and/or PFD. **C, G** RGS2 protein expression measured as the RGS2/β-actin protein ratio in HLF-9 (**C**) and NIH3T3 (**G**) treated with hUC-MSCs and/or PFD. Densities of bands were quantified using the ImageJ program. The results are presented as means ± SEM (n = 3). **D, H** HLF-9 and NIH3T3 cells were treated with TGF-β1 (4 ng/ml) firstly. Then, the Fluo-3 fluorescence of intracellular Ca²⁺ level in HLF-9 (**D**) and NIH3T3 (**H**) cells treated with PFD and/or hUC-MSCs were measured. The cells were excited at 488 nm and Ca²⁺-bound Fluo-3 emission was recorded at 530 nm. The Fluo-3 fluorescence from three separate exeachiments was plotted as means ± SEM. **I, J** HLF-9 (**I**) and NIH3T3 (**J**) were single cultured or co-cultured with hUC-MSCs, treated with 8 mM PFD for 24 h, and were then harvested for RT-PCR analysis of fibrosis marker mRNA levels. Values are means ± SEM (n = 3). **K** hUC-MSCs were treated with 4 ng/ml TGF-β1 and cultured for 24 h, treated with 8 mM PFD or an equal amount of PBS buffer for 24 h, and were then harvested for RT-PCR analysis of E-cad, FN, α-SMA mRNA levels. Values are means ± SEM (n = 3). *p < 0.05; **p < 0.01; ***p < 0.01

effects on pulmonary fibrosis and, in contrast to our expectations, the highest dose of PFD (300 mg/kg) did not achieve better antifibrotic effects than the medium dose (100 mg/kg). In the clinical trials of PFD for IPF conducted by Azuma A et al. and Wijsenbeek et al., the adverse effects of PFD included predominantly gastrointestinal reaction and were positively correlated with dose, with an incidence of 40–60%, and some patients discontinued the drug due to intolerance [30, 31]. Combined with the observation that the appetite of mice in the high-dose PFD group was poorer than in the medium- and low-dose PFD groups, it can be assumed that the PFD dose exceeded the ideal range, resulting in gastrointestinal adverse reactions and reducing the therapeutic effect of PFD. Therefore, we cannot expect to achieve a better antifibrotic effect by increasing the dose of PFD in clinical practice. For this reason, to avoid the adverse effects of higher doses of PFD, a combination of the low-dose

30 mg/kg PFD, with hUC-MSCs was used in this study instead of 100 mg/kg PFD with hUC-MSCs.

The pathogenesis of IPF remains unclear, but the main pathological changes are the proliferation and aggregation of large numbers of MFBs and the deposition of extracellular matrix, of which the main component is collagen [32]. MFBs, as the main effector cell of IPF, have a negative correlation with the severity and prognosis of IPF disease [26]. It was found that, in addition to their antifibrotic effects, hUC-MSCs have a certain degree in profibrotic effects, especially in the fibrotic environment, and can be converted to MFBs through endothelial–mesenchymal conversion [33, 34]. This may be one of the reasons for the controversial effects of hUC-MSCs in the treatment of pulmonary fibrosis. Furthermore, PFD, as a multi-cytokine inhibitor, can inhibit the expression of cytokines, such as TGF-β1, basic fibroblast growth factor (bFGF), and connective tissue growth factor (CTGF) of



target cells (myo)fibroblasts, suppressing the proliferation of (myo)fibroblasts and the synthesis of collagen [35, 36]. Therefore, in this study, we examined the changes in mRNA levels of EMT markers in hUC-MSCs. The results showed that E-cad mRNA was significantly increased, and FN and α -SMA mRNA expression were both significantly decreased after treatment of hUC-MSCs with PFD. This result indicated that PFD inhibited the conversion of hUC-MSCs to mesenchymal cells. In addition, RGS2 has a negative regulatory effect on EMT and can inhibit the conversion of fibroblasts to MFBs [37]. We found that RGS2 expression increased and markers of MFBs decreased in hUC-MSCs after treatment with PFD. The experimental results indicate that PFD treatment of hUC-MSCs can reduce the conversion of hUC-MSCs to MFBs, which gives hUC-MSCs the opportunity to maximize their antifibrotic effects. This may be one of the mechanisms by which hUC-MSCs combined with PFD can achieve better efficacy compared with PFD alone.

Many studies show RGS2 plays an important role in regulating the pathogenesis of fibrosis [18, 19]. In our study, we found RGS2 increased in hUC-MSCs combined PFD mice and MFBs and we assumed that the combination of the two treatments might exert antifibrotic effects through upregulation of PFD. It has been reported that

overexpression of RGS2 significantly reduces the expression of fibrosis markers and thus plays a protective role against pulmonary fibrosis [4], this result that could support our hypothesis. Previous literature reported that siRNA can knockdown the expression of endogenous RGS2 in cells [24]. In our experiments, we similarly used siRNA to knockdown RGS2 expression in NIH3T3. Our data showed that after RGS2 knockdown, PFD treatment and PFD combined with hUC-MSCs had no effect on the increase in fibrosis markers induced by TGF- β 1. Interestingly, there is also evidence that PFD treatment significantly upregulated endogenous lung RGS2 expression in RGS2^{+/+} mice. More importantly, their data showed a significant increase in collagen deposition in the lungs of bleomycin-treated RGS2 knockout mice compared to that in wild-type mice [4]. Another study showed RGS2 plays a protective role and that loss of RGS2 accelerates the progression of kidney fibrosis [18]. Those all suggests that upregulating RGS2 is a key mediator of antifibrotic effects associated with PFD and/or hUC-MSCs treatment.

RGS2 is a known negative regulator of G protein signaling that inhibits the amplitude and duration of signals mediated by Gq-coupled G protein-coupled receptors (GPCRs) [38, 39]. Several Gq-coupled GPCRs and their

ligands are important drivers of pulmonary fibrosis, including Gq-coupled proteinase-activated receptor 1 (PAR1), lysophosphatidic acid receptor 1, and endothelin receptor [40–43], which promote fibroblast proliferation and differentiation into an MFBs phenotype and promote the development of pulmonary fibrosis [43, 44]. Previous studies have shown that fibroblast proliferation is dependent on PAR1-mediated increases in intracellular Ca^{2+} [45, 46]. Increased intracellular Ca^{2+} concentration promotes fibroblast proliferation [27], induces fibroblast-to-MFBs conversion [47], leads to apoptosis of type II lung cells [48], and ultimately leads to the formation of pulmonary fibrosis. Therefore, GPCR-mediated Ca^{2+} signaling is closely related to IPF pathology. BLM increases Ca^{2+} signaling in MFBs in animal models [49]; in contrast, at the cellular assay level, TGF- β 1 increases Ca^{2+} signaling in MFBs [50]. Therefore, reducing intracellular Ca^{2+} levels may be a promising approach to preventing or ameliorating the progression of pulmonary fibrosis. RGS2 functions as a selective modulator of Gq-mediated signaling [38, 39, 51], which can reduce intracellular Ca^{2+} levels by negatively regulating G protein signaling [4]. The results of our experiments showed that, compared with PFD and hUC-MSC treatment alone, the combination of hUC-MSCs and PFD increased RGS2 protein levels, significantly decreased intracellular Ca^{2+} concentration, and significantly reduced fibrosis markers. We found that hUC-MSC and PFD treatment significantly reduced TGF- β 1-stimulated intracellular Ca^{2+} signaling which provides a molecular mechanism to explain the antifibrotic effects of RGS2.

Interestingly, our data demonstrated that RGS2 expression in hUC-MSCs and PFD was increased more than in the PFD-only treated group, and the role of hUC-MSCs in this phenomenon required further investigation. Previous studies have shown that Ca^{2+} signaling was closely associated with IPF pathology [49]. Therefore, reducing intracellular Ca^{2+} levels may be a promising approach to preventing or ameliorating the progression of pulmonary fibrosis. Li Q et al. demonstrated that hUC-MSCs could reduce intracellular Ca^{2+} concentrations [52]. PFD can attenuate thrombin-induced increases in intracellular Ca^{2+} by upregulating RGS2 [4]. We found that intracellular Ca^{2+} was significantly reduced in the hUC-MSCs combined with PFD group. Therefore, hUC-MSCs may synergize with PFD to reduce intracellular Ca^{2+} and produce stronger antifibrotic effects. Studies have shown that increased intracellular Ca^{2+} inhibits MSCs proliferation and promotes MSCs differentiation [53]. Therefore, lowering intracellular Ca^{2+} promotes MSCs proliferation and reduces MSCs differentiation, thereby maintaining more durable stem cell properties and facilitating

antifibrotic effects. In addition, hUC-MSCs exert antifibrotic effects mainly through paracrine secretion [12, 13]. Therefore, we speculate that hUC-MSCs increase the expression of RGS2 in MFBs through paracrine secretion of some substances and synergize with PFD to further elevate RGS2, thereby achieving a more antifibrotic effect. More research is needed to test this hypothesis.

Conclusion

In conclusion, the results of the present study provide direct evidence that hUC-MSCs combined with low-dose PFD had a therapeutic effect on a mouse model of pulmonary fibrosis and delayed the progression of IPF, providing new prospects for the clinical treatment of IPF. In addition, this study found that the possible mechanism of the efficacy of hUC-MSCs in combination with low-dose PFD may be related to a significant increase in the expression of the antifibrotic protein RGS2; however, the in-depth mechanism of the combined treatment should be further studied and explored.

Supplementary Information

The online version contains supplementary material available at <https://doi.org/10.1186/s12931-022-02192-6>.

Additional file 1: Table S1. Basic data of the number of dead mice treated with different doses of PFD. **Table S2.** Basic data of the number of dead mice treated with PFD and hUC-MSCs. **Figure S1.** Flow cytometry detection of surface mesenchymal stem cell markers of hUC-MSCs. **Figure S2.** The primitive view of the differentiation of hUC-MSCs. **A:** hUC-MSCs differentiated into chondrogenic cells. **B:** hUC-MSCs differentiated into osteogenic cells. **C:** hUC-MSCs differentiated into adipogenic cells. **Figure S3.** The Fluo-3 fluorescence intensity of Ca^{2+} levels in different group of HLF-9 were shown: H + T(A), H + T + M(B), H + T + P(C); H + T + M + P(D). Values are means \pm SEM (n = 3). * p < 0.05; ** p < 0.01; *** p < 0.01. **Figure S4.** The Fluo-3 fluorescence intensity of Ca^{2+} levels in different group of NIH3T3 were shown: N + T(A), N + T + M(B), N + T + P(C); N + T + M + P(D). Values are means \pm SEM (n = 3). * p < 0.05; ** p < 0.01; *** p < 0.01.

Acknowledgements

We gratefully acknowledge Dr. Huafeng Pan at Chongqing Stem Cell Therapy Engineering Technology Research Center for providing hUC-MSCs.

Author contributions

XW, and ZF participated in research design. XW, HG, HJQ and OZ conducted experiments. XW, HG, OZ and HJQ contributed materials and reagents. XW performed data analysis. XW, HML, ZF and LNC wrote or contributed to the writing of the manuscript. All authors read and approved the final manuscript.

Funding

This work was supported by National Nature Science Foundation of China (NSFC 81670018), Key project from Chinese Ministry of Science and Technology (2016YFA0101300) and the Science & Technology department of Sichuan Province (22ZDZX0014 and 2020YFS0105).

Availability of data and materials

All data generated or analyzed during this study are included in this published article and its Additional file 1.

Declarations

Ethics approval and consent to participate

No human participants, human data or human tissue involved in studies reported in this manuscript. All animal studies were approved by the Animal Ethics Committee of Chongqing Medical University.

Consent for publication

Not applicable.

Competing interests

The authors declare that they have no competing interests.

Author details

¹Division of Pediatric Pulmonology and Immunology, West China Second University Hospital, Sichuan University, Chengdu 610041, Sichuan, China. ²Key Laboratory of Birth Defects and Related Diseases of Women and Children, Sichuan University, Ministry of Education, Chengdu 610041, Sichuan, China. ³NHC Key Laboratory of Chronobiology, Sichuan University, Chengdu 610065, Sichuan, China. ⁴Hospital of Chengdu University of Traditional Chinese Medicine, Chengdu 610075, Sichuan, China. ⁵Pediatric Research Institute, Ministry of Education Key Laboratory of Child Development and Disorders, Children's Hospital of Chongqing Medical University, Chongqing 400015, China. ⁶Department of Respiratory Medicine, Children's Hospital of Chongqing Medical University, Chongqing 400015, China. ⁷Chongqing Engineering Research Center of Stem Cell Therapy, Chongqing 400015, China.

Received: 31 March 2022 Accepted: 22 September 2022

Published online: 01 October 2022

References

- Raghu G, Rochweg B, Zhang Y, Garcia CA, Azuma A, Behr J, et al. An official ATS/ERS/JRS/ALAT clinical practice guideline: treatment of idiopathic pulmonary fibrosis. An update of the 2011 clinical practice guideline. *Am J Respir Crit Care Med*. 2015;192(2):e3–19.
- Raghu G, Chen SY, Yeh WS, Maroni B, Li Q, Lee YC, et al. Idiopathic pulmonary fibrosis in US medicare beneficiaries aged 65 years and older: incidence, prevalence and survival, 2001–11. *Lancet Respir Med*. 2014;2:566–72.
- Hutchinson J, Fogarty A, Hubbard R, McKeever T. Global incidence and mortality of idiopathic pulmonary fibrosis: a systematic review. *Eur Respir J*. 2015;46(3):795–806.
- King TE Jr, Bradford WZ, Castro-Bernardini S, Fagan EA, Glassberg MK, et al. A Phase 3 trial of pirfenidone in patients with idiopathic pulmonary fibrosis. *N Engl J Med*. 2014;37:2083–92.
- Noble PW, Albera C, Bradford WZ, Costabel U, Glassberg MK, Kardatzke D, et al. Pirfenidone in patients with idiopathic pulmonary fibrosis (CAPACITY): two randomised trials. *Lancet*. 2011;377:1760–9.
- Ding DC, Chang YH, Shyu WC, Lin SZ. Human umbilical cord mesenchymal stem cells: a new era for stem cell therapy. *Cell Transplant*. 2015;24(3):339–47.
- Crisan M, Yap S, Casteilla L, Chen CW, Corselli M, Park TS, et al. A perivascular origin for mesenchymal stem cells in multiple human organs. *Cell Stem Cell*. 2008;3(3):301–13.
- Bianco P. "Mesenchymal" stem cells. *Annu Rev Cell Dev Biol*. 2014;30:677–704.
- Chang YS, Ahn SY, Yoo HS, Sung SI, Choi SJ, Oh WI, et al. Mesenchymal stem cells for bronchopulmonary dysplasia: Phase 1 dose-escalation clinical trial. *J Pediatr*. 2014;64(5):966–72.
- Fanping M, Ruonan X, Siyu W, Zhe X, Chao Z, Yuanyuan L, et al. Human umbilical cord-derived mesenchymal stem cell therapy in patients with COVID-19: a phase 1 clinical trial. *Signal Transduct Target Therapy*. 2020;5(1):172.
- Wilson JG, Liu KD, Zhuo H, Caballero L, McMillan M, Fang X, et al. Mesenchymal stem (stromal) cells for treatment of ARDS: a phase 1 clinical trial. *Lancet Respir Med*. 2015;3(1):24–32.
- Reddy M, Fonseca L, Gowda S, Chougule B, Hari A, Totey S. Human adipose-derived mesenchymal stem cells attenuate early stage of bleomycin induced pulmonary fibrosis: comparison with pirfenidone. *Int J Stem Cells*. 2016;9:192–206.
- Moodley Y, Atienza D, Manuelpillai U, Samuel CS, Tchongue J, Ilancheran S, et al. Human umbilical cord mesenchymal stem cells reduce fibrosis of bleomycin induced lung injury. *Am J Pathol*. 2009;175:303–13.
- Danyi P. Combination of human umbilical cord mesenchymal stem cells and nintedanib ameliorates mice pulmonary fibrosis induced by bleomycin. Chongqing, Chongqing Medical University, 2017.
- Hong Z, Chundi L, Lina L, Junying L, Yinghui G, Kun M, et al. Baicalin alleviates bleomycin-induced pulmonary fibrosis and fibroblast proliferation in rats via the PI3K/AKT signaling pathway. *Mol Med Rep*. 2020;21(6):2321–34.
- Tresa G, Mainak C, Mark AG, Robert N. A bronchoprotective role for Rgs2 in a murine model of lipopolysaccharide-induced airways inflammation. *Allergy Asthma Clin Immunol*. 2018;14:40.
- Jiang H, Xie Y, Abel PW, Wolff DW, Toews ML, Panettieri RA Jr, et al. RGS2 repression exacerbates airway hyperresponsiveness and remodeling in asthma. *Am J Respir Cell Mol Biol*. 2015;53:42–9.
- Jang HS, Kim JI, Noh M, Rhee MH, Park KM. Regulator of G protein signaling 2 (RGS2) deficiency accelerates the progression of kidney fibrosis. *Biochim Biophys Acta*. 2014;1842(9):1733–41.
- Peng Z, Jialin S, Michelle EK, Angel EM, Cindy P, Ulrike M. Regulator of G protein signaling 2 is a functionally important negative regulator of angiotensin II-induced cardiac fibroblast responses. *Am J Physiol Heart Circ Physiol*. 2011;301(1):H147–56.
- Xie Y, Jiang H, Zhang Q, Mehrotra S, Abel PW, Toews ML, et al. Upregulation of RGS2: a new mechanism for pirfenidone amelioration of pulmonary fibrosis. *Respir Res*. 2016. <https://doi.org/10.1186/s12931-016-0418-4>.
- Ashcroft T, Simpson JM, Timbrell V. Simple method of estimating severity of pulmonary fibrosis on a numerical scale. *J Clin Pathol*. 1988;41:467–70.
- Hua Z, Yi X, Yunqiu X, Rong Z, Daiyin T, Ting W, et al. Therapeutic effects of human umbilical cord-derived mesenchymal stem cells in acute lung injury mice. *Sci Rep*. 2017;7:39889.
- Zhang Y. The investigation of human umbilical cord mesenchymal stem cells on pulmonary fibrosis mice models. Chongqing, Chongqing Medical University, 2015.
- Zhang W, Anger T, Su J, Hao J, Xu X, Zhu M, et al. Selective loss of fine tuning of Gq/11 signaling by RGS2 protein exacerbates cardiomyocyte hypertrophy. *J Biol Chem*. 2006;281:5811–20.
- Fernandez IE, Eickelberg O. New cellular and molecular mechanisms of lung injury and fibrosis in idiopathic pulmonary fibrosis. *Lancet*. 2012;18;380(9842):680–8.
- Enomoto N, Suda T, Kato M, Kaida Y, Nakamura Y, Imokawa S, et al. Quantitative analysis of fibroblastic foci in usual interstitial pneumonia. *Chest*. 2006;130(1):22–9.
- Yu WK, Hwang WL, Wang YC, Tsai CC, Wei YH. Curcumin suppresses TGF- β -induced myofibroblast differentiation and attenuates angiogenic activity of orbital fibroblasts. *Int J Mol Sci*. 2021;22(13):6829.
- Kang QJ, Peng XD, Li XS, Hu DH, Wen GX, Wei ZQ, et al. Calcium channel protein ORAI1 mediates TGF- β induced epithelial-to-mesenchymal transition in colorectal cancer cells. *Front Oncol*. 2021;11: 649476.
- Oku H, Shimizu T, Kawabata T, Nagira M, Hikita I, Ueyama A, et al. Antifibrotic action of pirfenidone and prednisolone: different effects on pulmonary cytokines and growth factors in bleomycin-induced murine pulmonary fibrosis. *Eur J Pharmacol*. 2008;590:400–8.
- Azuma A, Nukiwa T, Tsuboi E, Suga M, Abe S, Nakata K, et al. Double-blind, placebo-controlled trial of pirfenidone in patients with idiopathic pulmonary fibrosis. *Am J Respir Crit Care Med*. 2005;171:1040–7.
- Wijsenbeek MS, Grutters JC, Wuyts WA. Early experience of pirfenidone in daily clinical practice in Belgium and the Netherlands: a retrospective cohort analysis. *Adv Therapy*. 2015;32:691–704.
- Thomas AW, Thirumalai RR. Mechanisms of fibrosis: therapeutic translation for fibrotic disease. *Nat Med*. 2012;18(7):1028–40.
- Gazdhar A, Grad I, Tamò L, Gugger M, Feki A, Geiser T. The secretome of induced pluripotent stem cells reduces lung fibrosis in part by hepatocyte growth factor. *Stem Cell Res Ther*. 2014;5:123.
- Mezey E. The therapeutic potential of bone-marrow-derived stromal cells. *J Cell Biochem*. 2011;112(10):2683–7.

35. Oku H, Shimizu T, Kawabata T, Nagira M, Hikita I, Ueyama A, et al. Antifibrotic action of pirfenidone and prednisolone: different effects on pulmonary cytokines and growth factors in bleomycin-induced pulmonary fibrosis. *Eur J Pharmacol.* 2008;20:400–8.
36. Myllarniemi M, Kaarteenaho R. Pharmacological treatment of idiopathic pulmonary fibrosis preclinical and clinical studies of pirfenidone, nintedanib, and N-acetylcysteine. *Eur Clin Respir J.* 2015;10:2.
37. Alsafadi DB, Abdullah MS, Bawadi R, Ahrum M. The association of RGS2 and slug in the androgen-induced acquisition of mesenchymal features of breast MDA-MB-453 cancer cells. *Endocr Res.* 2022;47(2):64–79.
38. Bernstein LS, Ramineni S, Hague C, Cladman W, Chidiac P, Levey AI, et al. RGS2 binds directly and selectively to the M1 muscarinic acetylcholine receptor third intracellular loop to modulate Gq/11alpha signaling. *J Biol Chem.* 2004;279:21248–56.
39. Heximer SP, Watson N, Linder ME, Blumer KJ, Hepler JR. RGS2/G0S8 is a selective inhibitor of Gαq function. *Proc Natl Acad Sci USA.* 2008;94:14389–93.
40. Shahar I, Fireman E, Topilsky M, Grief J, Schwarz Y, Kivity S, et al. Effect of endothelin-1 on alpha-smooth muscle actin expression and on alveolar fibroblasts proliferation in interstitial lung diseases. *Int J Immunopharmacol.* 1999;21:759–75.26.
41. Tager AM, LaCamera P, Shea BS, Campanella GS, Selman M, Zhao Z, et al. The lysophosphatidic acid receptor LPA1 links pulmonary fibrosis to lung injury by mediating fibroblast recruitment and vascular leak. *Nat Med.* 2008;14:45–54.
42. Königshoff M, Dumitrascu R, Udalov S, Amarie OV, Reiter R, Grimminger F, et al. Increased expression of 5-hydroxytryptamine2A/B receptors in idiopathic pulmonary fibrosis: a rationale for therapeutic intervention. *Thorax.* 2010;65:949–55.
43. José RJ, Williams AE, Chambers RC. Proteinase-activated receptors in fibroproliferative lung disease. *Thorax.* 2014;69:190–2.
44. Bogatkevich GS, Tourkina E, Silver RM, Ludwicka-Bradley A. Thrombin differentiates normal lung fibroblasts to a myofibroblast phenotype via the proteolytically activated receptor-1 and a protein kinase C-dependent pathway. *J Biol Chem.* 2001;276:45184–92.
45. Bachhuber BG, Sarembock IJ, Gimple LW, McNamara CA, Owens GK. Thrombin-induced mitogenesis in cultured aortic smooth muscle cells requires prolonged thrombin exposure. *Am J Physiol.* 1995;268:C1141–7.
46. Ide J, Aoki T, Ishivata S, Glusa E, Strukova SM. Proteinase-activated receptor agonists stimulate the increase in intracellular Ca²⁺ in cardiomyocytes and proliferation of cardiac fibroblasts from chick embryos. *Bull Exp Biol Med.* 2007;144:760–3.
47. Vlahakis SR, Villasis-Keever A, Gomez T, Vanegas M, Vlahakis N, Paya CV. G protein-coupled chemokine receptors induce both survival and apoptotic signaling pathways. *J Immunol.* 2002;169(10):5546–54.
48. Winters CJ, Koval O, Murthy S, Allamargot C, Sebag SC, Paschke JD, et al. CaMKII inhibition in type II pneumocytes protects from bleomycin-induced pulmonary fibrosis by preventing Ca²⁺-dependent apoptosis. *Am J Physiol Lung Cell Mol Physiol.* 2016;310(1):L86–94.
49. Zhao H, Li CD, Li LN, Liu JY, Gao YH, Mu K. Baicalin alleviates bleomycin-induced pulmonary fibrosis and fibroblast proliferation in rats via the PI3K/AKT signaling pathway. *Mol Med Rep.* 2020;21(6):2321–34.
50. Hsu WL, Hsieh YC, Yu HS, Yoshioka T, Wu CY. 2-Aminoethyl diphenylborinate inhibits bleomycin-induced skin and pulmonary fibrosis via interrupting intracellular Ca²⁺ regulation. *J Dermatol Sci.* 2021;103(2):101–8.
51. Ghavami A, Hunt RA, Olsen MA, Zhang J, Smith DL, Kalgaonkar S, et al. Differential effects of regulator of G protein signaling (RGS) proteins on serotonin 5-HT1A, 5-HT2A, and dopamine D2 receptor-mediated signaling and adenylyl cyclase activity. *Cell Signal.* 2004;16:711–21.
52. Li Q, Turdi S, Thomas DP, Zhou TJ, Ren J. Intra-myocardial delivery of mesenchymal stem cells ameliorates left ventricular and cardiomyocyte contractile dysfunction following myocardial infarction. *Toxicol Lett.* 2010;195(2–3):119–26.
53. Wu LZ, Zhang GR, Guo CG, Pan YP. Intracellular Ca²⁺ signaling mediates IGF-1-induced osteogenic differentiation in bone marrow mesenchymal stem cells. *Biochem Biophys Res Commun.* 2020;527(1):200–6.

Publisher's Note

Springer Nature remains neutral with regard to jurisdictional claims in published maps and institutional affiliations.

Ready to submit your research? Choose BMC and benefit from:

- fast, convenient online submission
- thorough peer review by experienced researchers in your field
- rapid publication on acceptance
- support for research data, including large and complex data types
- gold Open Access which fosters wider collaboration and increased citations
- maximum visibility for your research: over 100M website views per year

At BMC, research is always in progress.

Learn more biomedcentral.com/submissions

